YSSP Report
Young Scientists Summer Program

Emissions from metal production to meet renewable energy demand in climate scenarios

Sagar D. Rathod[1,3], Tami C. Bond[2], Zbigniew Klimont[3], Jeffrey R. Pierce[1], Natalie Mahowald[4], Chaitri P. Roy[5,1], John Thompson[6], Karin Olson Hoal[4], and Peter Rafaj[3]

[1]Department of Atmospheric Science, Colorado State University, Fort Collins, Colorado, USA
[2]Department of Mechanical Engineering, Colorado State University, Fort Collins, Colorado, USA
[3]International Institute for Applied Systems Analysis, Laxenburg, Austria
[4]Department of Earth and Atmospheric Science, Cornell University, Ithaca, New York, USA
[5]Indian Institute of Tropical Meteorology, Pune, Maharashtra, India
[6]PetraScience Consultants, Vancouver, BC, Canada

Approved by

Supervisor: Peter Rafaj
Program: Pollution Management
30th September 2021

Contents

This research was funded by IIASA and its National Member Organizations in Africa, the Americas, Asia, and Europe.

ZVR 524808900

Abstract

A shift from fossil fuel to renewable energy is crucial in achieving climate goals of 2 degrees Celsius. However, the renewable energy technologies, solar photovoltaics, wind turbines, and electric vehicles are metal-intensive, while the mining and smelting processes to obtain the relevant metals are emissions-intensive. We estimate future $PM_{2.5}$ emissions from mining and smelting to meet the metal demand of renewable energy technologies in two climate pathways to be around 0.3-0.6 Tg/yr in the 2030-2040 period, which could be around 10-30% of total anthropogenic $PM_{2.5}$ emissions in many countries in those years. The concentration of mineral reserves in a few regions means the impacts are also regionally concentrated. The regional distributions of global emissions relative to metal demand depend on the metal production regionality and emission abatement measures. Stronger emissions abatement could reduce metal-related emissions by over 90% and avoid emission hotspot creation.

Acknowledgments

I would like to thank the USA National Academy of Science, Engineering, and Medicine (a IIASA-NMO) for providing the funding during the course of the YSSP. I would like to thank Dr. Peter Rafaj, Dr. Zbigniew Klimont, and Dr. Tami Bond for their guidance and help during the project.

About the authors

Sagar Rathod is a Young Scientists Summer Program researcher at IIASA, and a PhD student in the Department of Atmospheric Sciences at the Colorado State University, Fort Collins, Colorado, USA; sagar.rathod@colostate.edu

Tami Bond is Professor in the Mechanical Engineering Department at the Colorado State University, Fort Collins, Colorado, USA; tami.bond@colostate.edu

Zbigniew Klimont is the Research Group Leader and Principal Research Scholar Pollution Management Research Group - Energy, Climate, and Environment Program at IIASA, Laxenburg, Austria; klimont@iiasa.ac.at

Jeffrey Pierce is Professor in the Department of Atmospheric Sciences at the Colorado State University, Fort Collins, Colorado, USA; jeffery.pierce@colostate.edu

Natalie Mahowald is Professor in the Department of Earth and Atmospheric Science, Cornell University, Ithaca, New York, USA; mahowald@cornell.edu

Chaitri Roy is Scientist at Indian Institute of Tropical Meteorology, Pune, Maharashtra, India; chaitri.cat@tropmet.res.in

John Thompson is Consultant at PetraScience Consultants, Vancouver, BC, Canada; jft66@cornell.edu

Karin Olson Hoal is Professor in the Department of Earth and Atmospheric Science, Cornell University, Ithaca, New York, USA; keo52@cornell.edu

Peter Rafaj Senior Research Scholar Pollution Management Research Group - Energy, Climate, and Environment Program at IIASA, Laxenburg, Austria; rafaj@iiasa.ac.at

1. Introduction

Anthropogenic emissions of greenhouse gases (GHGs) from fossil fuel combustion are the largest cause of climate change including global warming (Masson-Delmotte et al., 2021). Projections of future global warming due to ongoing human activities suggest a temperature increase of 2 to 6 degrees Celsius compared to pre-industrial levels (Masson-Delmotte et al., 2021). To limit this temperature increase, various countries have committed to reducing their greenhouse gas emissions by shifting their energy source to renewable energy such as solar and wind (“The Paris Agreement, UNFCCC, 2016”).

However, most of the renewable energy technologies are material intensive (Giurco et al., 2019; Watari et al., 2019) and require conventional (steel, aluminum, copper) and rare-earth (lithium, vanadium, neodymium) metals. The extraction and processing of these metals are emissions-intensive activities and have caused or are causing local and transboundary environmental damages (Csavina et al., 2011; Ghose & Majee, 2001; Kavouras et al., 2001). On a production basis, the major renewable energy technologies solar photovoltaics and wind turbines require more than two orders of magnitude more metals than fossil fuel technologies (Valero et al., 2018; Watari et al., 2019). Studies suggest the metal requirement to make the major renewable energy technologies including electric vehicles (EVs) might reach around 5-20 times the present-day levels in 2050 (e.g. Giurco et al., 2019). Mining and smelting are two major metal-related processes to bring them into the economy. Both these processes are emissions-intensive for air-quality relevant species such as particulate matter and SO_2 (Dudka & Adriano, 1997). Mining-related emissions occur during digging and extraction in open-pit mines, loading and unloading from trucks to storage, storage and handling, and some initial ore refinement at source (cutting or crushing, wetting, etc) (Ghose & Majee, 2001; Huertas et al., 2012). Smelting-related emissions occur during high-temperature melting of metals to reduce impurities (generally in a blast furnace) and some secondary melting with high-grade oxygen to reach desired quality (generally in a basic oxygen furnace or in the presence of some electrolytes) (US EPA, 2016). In terms of primary impacts, mining and smelting contribute to more than 10% of ambient $PM_{2.5}$ concentrations in various industrial cities such as Santiago in Chile and Panzhihua in China and in countries such as Germany (Jorquera & Barraza, 2012; Klimont et al., 2002; Xue et al., 2010). Besides, metal smelting is also a cause of heavy-metal pollution, such as mercury and nickel, in many places (Tian et al., 2012; Wu et al., 2012). However, there is no estimation of future impacts on air quality from the processes to obtain these materials.

More than 20 metals are required in the production of solar PVs, wind turbines, and EVs. Only a few countries have economically feasible reserves and resources of many of these metals, and hence these countries control the metals supply (e.g. Giurco et al., 2019). For example, the Bolivia-Argentina-Chile triangle has over 50% of known reserves of lithium, a critical metal for batteries (Seefeldt, 2020). However, along with supplying the metals, these regions also bear the environmental impacts from mining and smelting (Kaunda, 2020). The dependence on solar and wind for rapid decarbonization and the material intensity of these technologies and the subsequent environmental impacts hence create a complex problem: global decarbonization might create local pollution impacts (Lèbre et al., 2020; Mwaanga et al., 2019). However, as countries move toward becoming independent in terms of their critical mineral stock or acquiring raw ores for local processing into finished products, it could lead to changes in where impacts might occur (e.g. Round Top Mountain, USA, Pingitore, 2019).

In this work, we estimate primary $PM_{2.5}$ emissions from mining and smelting of metals obtained specifically for making three technologies related to renewable energy – solar PV, wind turbines, and EVs. We then contrast the regional distribution in metal demand (regions creating a metal demand by adding renewable energy capacity) and supply (regions producing metals) as well as emissions to estimate how regionally concentrated are impacts compared to the demand.

2. Methods

We estimate the atmospheric emissions of $PM_{2.5}$ (particulate matter with diameter smaller than 2.5μm) by multiplying activity (drivers that cause emissions, such as energy or amount of metal mined) and emission factors (emission intensities of processes including abatement) (Bond et al., 2004; Klimont et al., 2017).

Activity: We use the International Energy Agency's World Energy Outlook 2020 (IEA, 2020) projections of solar photovoltaics ('solar'), wind turbines ('wind') and electric vehicles ('EV') in their two scenarios, Stated Policies (termed here "Business-As-Usual") with GHG emissions similar to a Shared SocioEconomic Pathways (SSP) 3-7.0 scenario, and Sustainable Development (termed here "Rapid Decarbonization") with faster decarbonization than Business-As-Usual, GHG emissions similar to SSP 1-2.6. The selection of these two scenarios, which have different decarbonization rates, allows us to compare how the decarbonization rate affects metal demand, total anthropogenic emissions, the role of mining and smelting toward total air pollution, and the demand-supply-related regional distributions in the metal sector. Metal composition and intensities are used from Watari et al., (2019) for all the three technologies (Table S1). The metal intensities are assumed to remain constant throughout the 2020-2050 period but there could be possibilities of compact devices or devices that use different materials in future. For the mining sector, the activity is estimated as the sum of the steel, aluminum, and all non-ferrous metals multiplied by three (based on 2019 steel-to-iron-ore and aluminum-to-bauxite production ratios, BGS, 2019, USGS 2020) since the metal-to-ore data were scarce for most metals, and because many important critical metals are simply obtained as by-products during conventional metal production (BGS, 2019). In terms of scope, only the capacity (in GW for solar and wind) and fleet addition (in absolute numbers for EVs) are considered. Other factors such as modifying the grid structure and adding batteries for utility energy storage might represent a major fraction of metal demand (IEA, 2020) but these factors are not considered here. IEA data then are downscaled from the original 26 mega regions to 180 emission model regions using a downscaling routine described in SI Text 1. We also explore a 'Self-Producing' scenario in which a region produces metal to meet its own demand. This narrative allows us to analyze the effect of achieving the demand-supply equality on the demand-emissions distributions in the two decarbonization pathways.

Emission Factors: $PM_{2.5}$ emission factors are used from the GAINS (Greenhouse gas - Air pollution INteractions and Synergies, Klimont et al., 2017) model for the metal mining and smelting sectors. Two GAINS abatement pathways, "Projected Abatement" (abatement policies modeled based on current policies and trends) and "Strictest Abatement" (maximum feasible reduction pathways for emissions in future) are also analyzed. The major focus on this paper will be with Projected Abatement, and Strictest Abatement is used to assess the effect of stricter abatement policies on emissions. We only estimate primary $PM_{2.5}$ emissions in this work and not the precursor sulfate or nitrate emissions for which smelting operations are shown to be major contributors (e.g. Smith et al., 2011).

Thus, we analyze total eight cases: two decarbonization pathways (Business-As-Usual and Rapid Decarbonization), two abatement scenarios (Projected Abatement and Strictest Abatement), and two production regionalities (Actual and Self-Producing). The analysis is performed for the global scale for the years 2020 to 2050, with a 5-year resolution. We then use Equations 1, 2, and 3 to estimate metal demand from the IEA solar and wind capacity addition and EV fleet projections, map the metal demand to relevant GAINS process sectors, and estimate emissions from each GAINS sector in different years, respectively.

Equation 1: Estimating global metal demand

$$MD_{m,i,t,s} = \sum_{r=1}^{n} \Delta RAC_{i,t,r,s} * MI_{m,t} \quad \textbf{(1)}$$

Intermediate step: Mapping metal m to GAINS sector gs (how a metal production is representation in GAINS)

1. Steel: Basic Oxygen Furnace, Electric Arc Furnace, Open Hearth Furnace
2. Aluminum: Primary and Secondary smelting
3. Non-Fe, Non-Al ('NFME'): single sector representing all non-ferrous, non-aluminum metals
4. Mining: single sector representing all metal mining

Equation 2: Mapping metal demand to the producing region

Metal activity in region r in GAINS sector gs = Global metal demand * Fraction of all-use metal m produced in region r in GAINS sector gs

$$MC_{m,i,t,r,s,gs} = MD_{m,i,t,s} * \frac{MIEA_{m,i,t,s,gs,r}}{MIEA_{m,i,t,s,gs}} \quad \textbf{(2)}$$

Equation 3: Emissions

$$E_{m,i,t,r,s} = MC_{mi,t,r,s,gs} * EF_{i,gs,r} * (1 - ABAT_{i,gs,r}) \quad \textbf{(3)}$$

Equation 4 for Self-Producing case: Mapping of metal demand to GAINS sectors

$$MC_{m,i,t,r,s,gs} = MD_{m,i,t,r,s} * \frac{MIEA_{m,i,t,s,gs,r}}{MIEA_{m,i,t,s,r}}$$

Where m = metal, i = year, t = technology, r = region, s = scenario, ΔRAC = renewable energy capacity addition (GW/yr), MI = metal intensity of renewable energy technologies (e.g. ton metal / GW solar addition), MD = metal demand (ton / yr), MC = GAINS metal activity (ton / yr), c = country of region, MIEA = metal activity in IEA all-use projections (ton /yr), gs = GAINS sector (EARC, BAOX, etc), E = emissions (Gg/yr), EF = Emission Factor (Gg $PM_{2.5}$ / ton activity), ABAT = efficiency of control measures (dimensionless; $PM_{2.5}$ out / $PM_{2.5}$ in).

Unequal regional distribution of metal demand and production means only a few regions bear most of the emissions burden, and impacts are not necessarily felt where decarbonization occurs. It is thus important to understand how a regional or global policy on decarbonization causes disproportionately higher emissions elsewhere or leads to creation of emissions hotspots. We use the Gini framework (Gastwirth, 1972; Lorenz, 1905) to compare the regional distributions of emissions to metal demand in different scenarios. The Gini index represents how a variable is distributed compared to the other and has been used in social economics (e.g. population vs income distributions). The Gini index can be derived by plotting in Cartesian coordinates where the x-axis is the cumulative normalized rank of a variable A from the lowest to the highest and the y-axis is the cumulative normalized variable B from the lowest to the highest. Then, the Gini index can be calculated as the ratio of the area between the perfect equality line and the curve divided by the total area under the perfect equality line. A Gini value closer to zero would indicate emissions are occurring where demand is occurring. And a Gini value closer to one would indicate most emissions are comparatively more concentrated in fewer regions than demand is.

Hence, a total of 8 cases are studies in this work – two decarbonization scenarios with two abatement pathways, and two production regionalities (Table 1).

Table 1: Cases studies in this work

Decarbonization Scenario	Metal Production Regionality	Abatement on Metal-related processes
Business-As-Usual	Actual	Projected
Business-As-Usual	Actual	Strictest
Business-As-Usual	Self-Producing	Projected
Business-As-Usual	Self-Producing	Strictest
Rapid Decarbonization	Actual	Projected
Rapid Decarbonization	Actual	Strictest
Rapid Decarbonization	Self-Producing	Projected
Rapid Decarbonization	Self-Producing	Strictest

3. Results and Discussion

3.1 Metal demand

The estimated global metal demand is 100-500 million tons per year by solar, wind, and EVs in Business-As-Usual (IEA Stated Policies Scenario) and Rapid Decarbonization (IEA Sustainable Development Scenario) scenarios between 2020 and 2050 (Figure S1, Table S2). Metal demand is dominated by solar in all years in both the scenarios (Figure S1) due to its high metal intensity dominated by iron and steel, and the overall role in capacity addition. EVs pose around 20% of renewables-related metal demand in Business-As-Usual and 30% in Rapid Decarbonization. Total metal demand by wind turbines is the least, at around 1-4% in both the scenarios. Steel dominates the metal mix and demand, followed by aluminum and non-ferrous metals (Table S1 and S2). The metal demand toward renewables represents about 8-17% of all-use (metal use for construction, machinery, etc) demand for steel, 10-28% for non-ferrous metals, and 4-12% for aluminum (Table S2).

Regionally, low- and middle-income countries represent most of the metal demand due to their projected renewable energy addition (IEA, 2020). India and China account for 20-45% metal demand (Figure S2-S4) via solar, wind, and EVs. High-income regions represent a major demand in the first half of the 2020-2050 period but then have a slower growth, except for EVs where their growth is higher in the second half (Figure S2-S4). The relative metal demand is much higher from Asian, African, and Latin American countries in the Rapid Decarbonization than Business-As-Usual for all the three technologies, and Rapid Decarbonization in general has more regional diversity in demand than Business-As-Usual.

3.2 Emissions

Figure 1a and 1b show the absolute regional $PM_{2.5}$ emissions from mining and smelting to meet the metal demand of global renewables in the Business-As-Usual and Rapid Decarbonization pathways with the Projected Abatement measures. The Rapid Decarbonization values are almost twice as Business-As-Usual in many years for the Projected Abatement case, similar to metal demand. The emissions regionality in Business-As-Usual and Rapid Decarbonization is similar, with India and China dominating emissions in both. USA, Russia, Eastern Europe and rest-of-Asia account for about 30% of emissions. Non-India non-China Asian countries, African, and Latin American countries have similar contribution to emission in Business-As-Usual and Rapid Decarbonization. This is a deviation from metal demand, where these regions have a higher share in Rapid Decarbonization than Business-As-Usual.

Stronger abatement in future years could lead to almost 90% emissions reduction in both the pathways (Figure S5). Smelter plants in countries such as India might undergo rapid cleaning compared to other similar countries such as China, and hence its contribution between the two abatement scenarios could become much lower. However, because dominant regions in the Projected Abatement case such as India and China could clean up more in the Strictest Abatement (Maximum Feasible Reduction) case, the relative contribution from regions such as EU and USA could then become higher.

There are interesting patterns when the emissions are disaggregated by metals and processes. Technology-wise, Solar and EVs represent most of the emissions in Business-As-Usual and Rapid Decarbonization with both Projected Abatement and Strictest Abatement (Figure S6). Process-wise, smelting represents about 95% of total $PM_{2.5}$ emissions and mining the rest (Figure S6). Steel, non-Ferrous metals (NFMEs), and Aluminum smelting represent about 80%, 10%, and 5% of the total, with similar contributions in Projected Abatement and Strictest Abatement cases. However, as abatement selectively operates more on point sources in future years, the contribution of mining might increase even in the Strictest Abatement case (Figure S7). Using a single metal-to-ore ratio and a single emission factor for different mining process might contribute to a bias toward low emissions from mining. A point to note here is that as current mines run out of feasible, high-grade ores, economies might either shift production to newer, feasible mines (along with creating new smelter plants near them) or dig more to get the same ore amount (e.g. Mohr et al., 2015). Either of these mining choices might strongly affect where and how activity could occur in future.

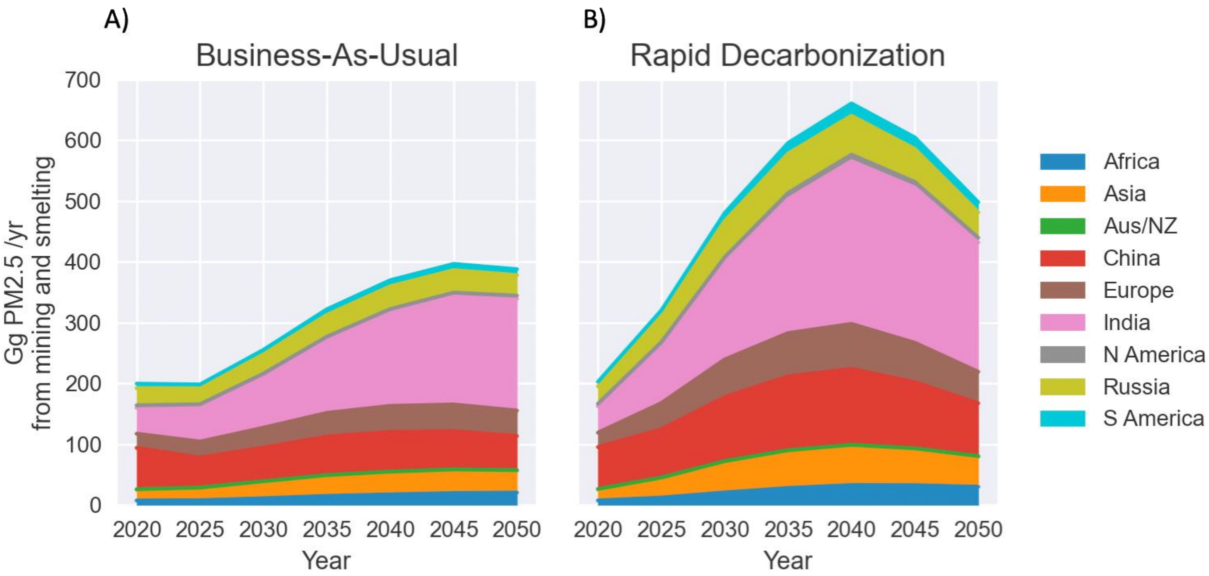

Figure 1: $PM_{2.5}$ emissions from metal mining and smelting toward making renewable energy devices in Business-As-Usual (a) and Rapid Decarbonization (b) scenarios by region with Projected Abatement policies.

Globally, the $PM_{2.5}$ emissions from mining and smelting to meet metal demand for renewables are small but most of these emissions occur in a few regions (Figure 1), and in an even smaller area (mostly near industrial cities or near mines) in those regions (e.g. Banza Lubaba Nkulu et al., 2018), hence a different set of population is affected. For context, the absolute emission values of 300-600 Gg/yr in Business-As-Usual and Rapid Decarbonization are around 5-10% of present-day global anthropogenic Black Carbon emissions or 2.5-5% of global industrial and power sector's $PM_{2.5}$ emissions (Klimont et al., 2017).

Figure 2 shows the absolute anthropogenic combustion and metal-related emissions in the two decarbonization scenarios, along with the percent contribution of mining and smelting to total anthropogenic emissions for India, China, and Rest of the World. $PM_{2.5}$ emissions from mining and smelting to meet global renewable energy demand could reach 5-15% of total anthropogenic combustion-related $PM_{2.5}$ emissions in India and China in both the decarbonization scenarios with Projected Abatement policies. $PM_{2.5}$ emission contribution due to mining and smelting is amplified in the Rapid Decarbonization scenario due to its faster decarbonization demanding more metals and hence emissions from metal sector and simultaneously reducing fossil fuel contribution. However, overall anthropogenic combustion $PM_{2.5}$ emissions are also lower in the Rapid Decarbonization scenario compared to Business-As-Usual, thus far more offsetting for the increased metal-related emissions, even with moderate abatement policies.

Detailed region-specific information is shown in Figures S8 and S9 for the Projected and Strictest Abatement policies, respectively. Metal-related and anthropogenic combustion $PM_{2.5}$ emissions in the Strictest Abatement case are much lower for most of the regions compared to Projected Abatement (Figure S9) especially after 2035 when the abatement differences in the two scenarios become larger. However, in regions such as Australia/New Zealand, Canada, USA, and Mexico, and China, abatement on other combustion processes might be stronger than on metal-related processes, making the relative contribution of the metal sector higher in Strictest Abatement than Projected Abatement (Figure S8 and S9).

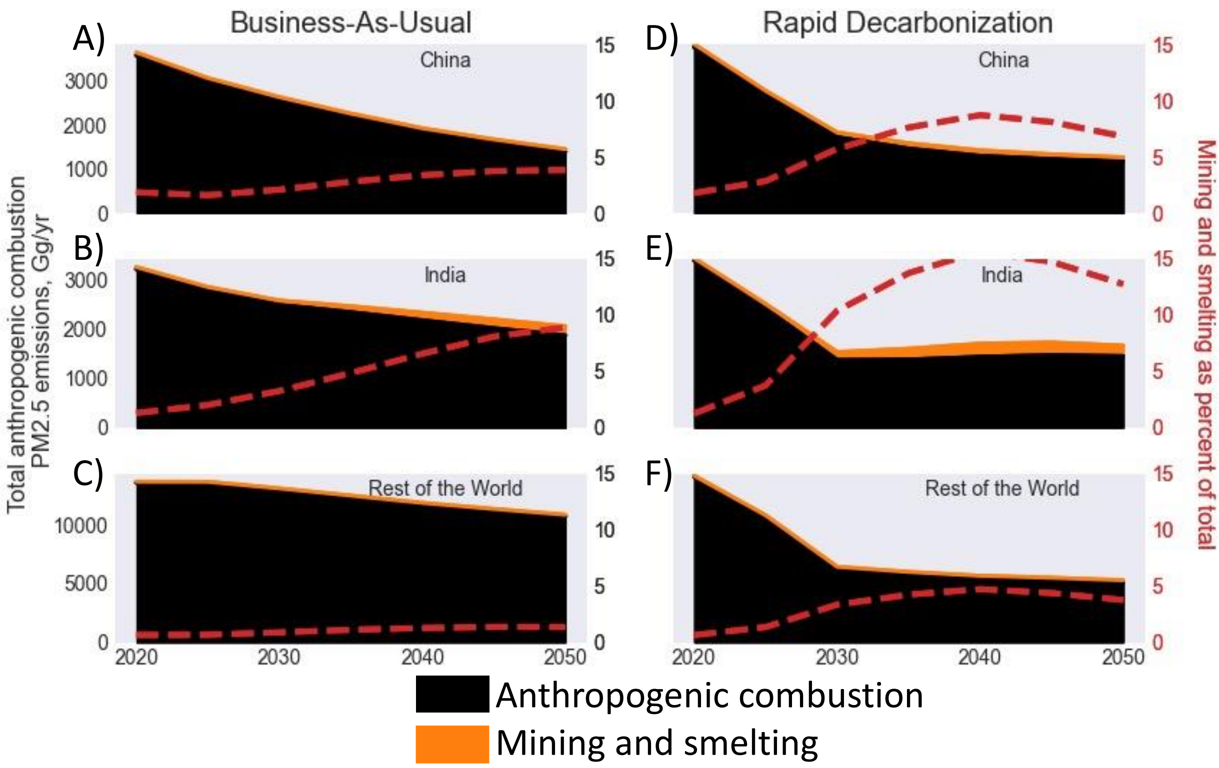

Figure 2: Absolute PM2.5 emissions from anthropogenic combustion (black) and mining and smelting for metals for renewable technologies (orange) shown for the Business-As-Usual and Rapid Decarbonization scenarios (left axis in A-F) for India, China, and Rest of the World. $PM_{2.5}$ emissions by mining and smelting to meet metal demand for renewables, shown as percent of total (mining and smelting and fossil fuel combustion) (red line, right axis in A-F).

3.3 Regional distributions of metal demand, production, and emissions

Figure 3a and 3b show the relative regional contributions to metal demand, production, and smelting-related $PM_{2.5}$ emissions in the two abatement scenarios for the Business-As-Usual and Rapid Decarbonization pathways for the year 2050 when Actual production regionality is considered. Most metal demand is driven by China, India, and rest of Asia and fulfilled in roughly similar proportions. However, emissions mainly occur in India if Projected Abatements are considered, and in China if Strictest Abatements are considered in both the decarbonization scenarios. This is only due to the differences in those region's emission factors and abatement measures. Other regions such as Russia and Europe have relatively lower metal demand but have higher contribution to production and hence also bear relatively higher emissions burden compared to their share in demand.

Figure 3c and 3d show the same information as 3a and 3b, for the 'Self-Producing' case where the demand-supply regionality is assumed to be the same. This case represents a world with a form of 'just' transition in which countries aim at keeping energy jobs and finance in their own countries by increasing investments in the renewables and hence the metal sector. Under this ‘self-producing’ assumption, contribution to emissions by Asian and African countries increases relative to the Actual production case. This is mainly due to their relatively higher emission factors and lower projected abatement. Under the Strictest Abatement, the GAINS model assumes faster reduction in India and China than the rest of Asia. Hence, the relative contribution by rest of Asia could dominate the global metals-related emissions. The demand and emissions in the Self-Producing narrative seems to be slightly evenly distributed compared to Actual when Projected Abatements are considered (Figure 3). However, emissions could probably get concentrated over fewer regions if Strictest Abatement measures are considered in the Self-Producing case.

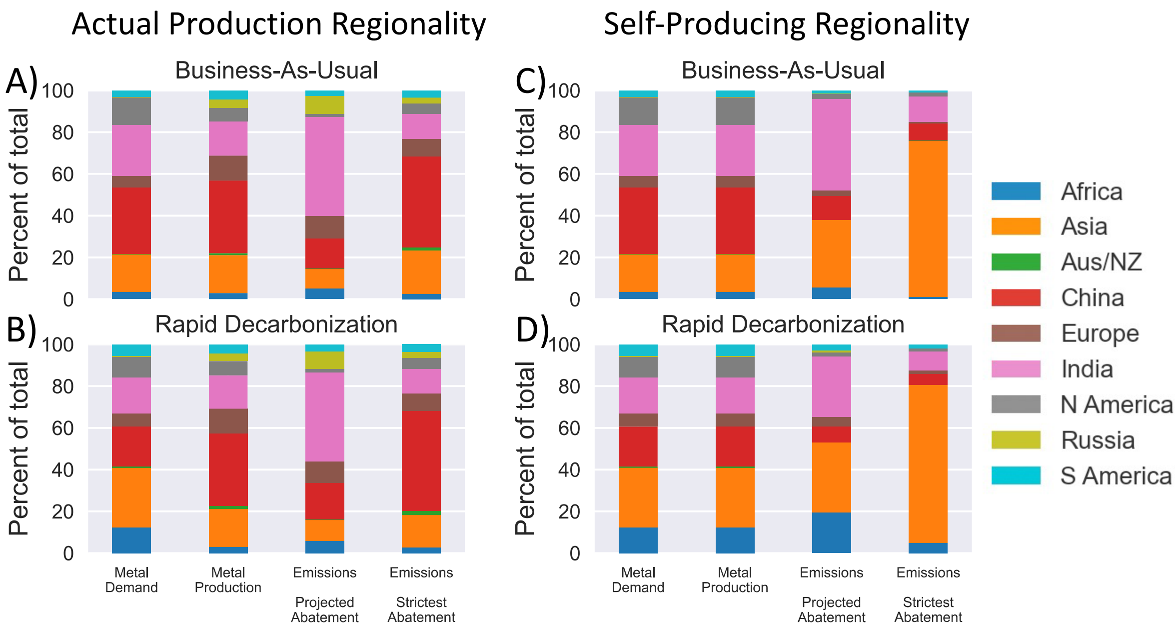

Figure 3: Percent of total metal demand, production, and related emissions aggregated across the three renewable technologies and all-metal smelting, for the Business-As-Usual and Rapid Decarbonization scenarios with Moderate Abatement policies with Actual supply regionality (a and b), and with supply regionality assumed to be same as demand regionality (c and d).

Figure 4 shows the Gini Index timeseries for the 8 cases studies in this work – two decarbonization scenarios with two abatement pathways, and two production regionalities (data in Table S3). Business-As-Usual cases are colored red and Rapid Decarbonization are colored green. The linewidths are proportional to the total emissions in each case. The Gini Index points to how evenly distributed are emissions relative to demand by region in each case (Columns 3 and 4 compared to Column 1 in Figure 3a-d). Regional distributions of emissions relative to the demand could become more even or uneven in time as different regions demand metals via their renewables addition programmes, their metal production capacity changes, and as they adopt different abatement policies to meet air quality targets. Strictest Abatement cases with Business-As-Usual and Rapid Decarbonization cases have lesser distributional differences than the Projected Abatement cases, indicating the important role of abatement policies in reducing concentration of emissions in a few regions. The demand-emissions distributions are more or less independent of the rate of decarbonization (Business-As-Usual versus Rapid Decarbonization) but probably depend on the abatement and production regionality considerations. The Self-Producing cases have relatively higher distributional differences (possibilities of more emission hotspots) than most Actual production cases. It is worth noting here that a 'just' transition goal should include two aspects: 1. Low overall global emissions from the metals sector, and 2. Low concentration of emissions and hence impacts in a few regions. However, in a scenario in which countries mine and smelt metals for their own renewables programme, it could lead to overall higher global emissions (Self-Producing cases having thicker lines in Figure 4 than Actual Production cases), along with concentration of emissions in fewer regions than in the real world where production is distributed because of comparative advantage based on labor and finance.

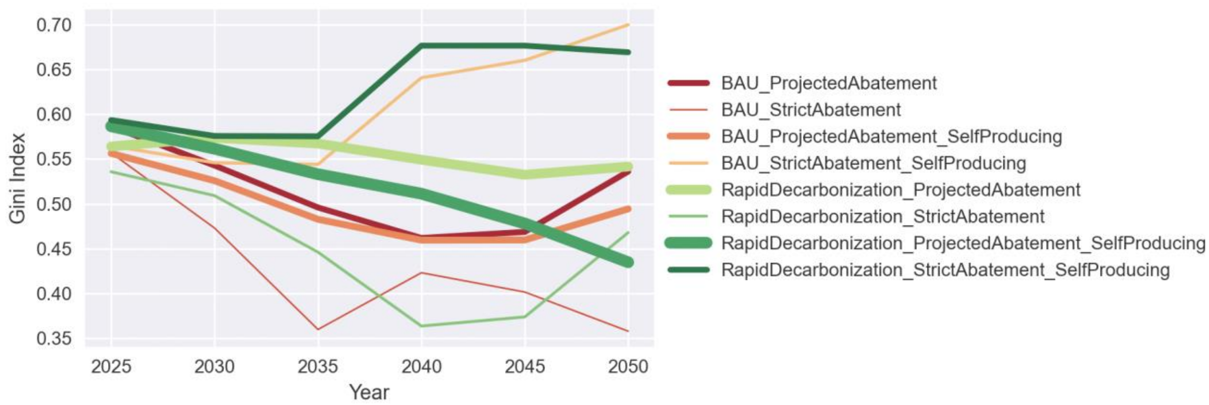

Figure 4: The Gini index trend for Demand-Emissions distributions for all the cases analyzed in this work. Linewidths are linearly proportional to 2025-2050 total emissions from smelting in each case. The Gini Index shows how regionally are emissions distributed compared to the where demand is happening. A Gini value closer to zero indicates emissions are occurring where demand is occurring. Values closer to one indicate most emissions are comparatively more concentrated in fewer regions than demand is. BAU = Business-As-Usual

The underlying cumulative distributions and their timeseries are shown in Figure S10-S18 for activity and emissions at various disaggregations. Solar, wind, and EVs have similar demand-production distribution for the Business-As-Usual and Rapid Decarbonization scenarios in almost all the years (Figure S10-S12), with the distribution being slightly more uneven in Rapid Decarbonization in some of the years. Non-Ferrous metals might have the most unevenly distributed demand-production regionality, followed by steel and aluminum (Figure S13-S15).

Demand and supply-related distributions could become more uneven in future as more regions demand renewable technologies in both the scenarios but only a few produce. The level of abatement also affects the demand-emissions distributions in the three technologies (Figure S16-S18). As stronger abatement in later years happens in many regions, it might progressively make the demand-emissions distributions more even for the solar PV and wind turbine technologies, but probably not for EVs (Figure S16-S18). Hence, stronger abatement could not only reduce overall emissions but also the overall inequality regardless of the activity pathway.

4. Summary and Conclusion

A shift from fossil fuel to renewable energy is crucial in achieving climate targets. However, the order of magnitude higher material intensity of most renewable energy devices compared to fossil fuel technologies, and the emission-intensive methods to obtain those materials generates environmental impacts at various spatial scales. This work quantifies the $PM_{2.5}$ emissions from mining and smelting due to metal requirement for achieving the renewable energy goals in two IEA scenarios. Total metal demand to make solar photovoltaics, wind turbines, and electric vehicles could reach around 100-500 million tons per year in future. This metal demand is estimated be around 8-17% of all-use values for steel and 10-28% for non-ferrous metals. The global $PM_{2.5}$ emissions from mining and smelting to meet the renewable energy sector's metal demand is estimated to reach around 300-600 Gg/yr some of the future years, representing about 5% of present-day industrial and power generation-related $PM_{2.5}$ emissions. India and China are projected to bear most of the $PM_{2.5}$ emissions burden to make metals for renewable energy regardless of the abatement levels. $PM_{2.5}$ emissions from mining and smelting could reach about 15% of combustion-related $PM_{2.5}$ emissions in many regions in a conservative scenario, and about 30% in the rapid decarbonization scenario. However, only a small number of regions produce most of the metals. The distributions of emissions by regions compared to metal-demanding regions could become more uneven in future but depends on the decarbonization rate, abatement policies, and where production happens. Stricter abatement levels could aid in decreasing the metal demand-emissions-related distributions along with decreasing overall anthropogenic emissions. A hypothetical scenario where countries produced metals for their own demand was also explored as a notion of demand-production equality. If all countries mined and smelted to meet their own metal demand, it could lead to overall higher global emissions and more uneven regional distributions of emissions relative to the Actual production case, where production is distributed based on comparative advantage.

References

Banza Lubaba Nkulu, C., Casas, L., Haufroid, V., De Putter, T., Saenen, N. D., Kayembe-Kitenge, T., et al. (2018). Sustainability of artisanal mining of cobalt in DR Congo. *Nature Sustainability*, *1*(9), 495–504. https://doi.org/10.1038/s41893-018-0139-4

Bond, T. C., Streets, D. G., Yarber, K. F., Nelson, S. M., Woo, J.-H., & Klimont, Z. (2004). A technology-based global inventory of black and organic carbon emissions from combustion. *Journal of Geophysical Research: Atmospheres*, *109*(D14). https://doi.org/10.1029/2003JD003697

Csavina, J., Landázuri, A., Wonaschütz, A., Rine, K., Rheinheimer, P., Barbaris, B., et al. (2011). Metal and Metalloid Contaminants in Atmospheric Aerosols from Mining Operations. *Water, Air, & Soil Pollution*, *221*(1), 145–157. https://doi.org/10.1007/s11270-011-0777-x

Dudka, S., & Adriano, D. C. (1997). Environmental Impacts of Metal Ore Mining and Processing: A Review. *Journal of Environmental Quality*, *26*(3), 590–602. https://doi.org/10.2134/jeq1997.00472425002600030003x

Gastwirth, J. L. (1972). The Estimation of the Lorenz Curve and Gini Index. *The Review of Economics and Statistics*, *54*(3), 306–316. https://doi.org/10.2307/1937992

Ghose, M. K., & Majee, S. R. (2001). Air pollution caused by opencast mining and its abatement measures in India. *Journal of Environmental Management*, *63*(2), 193–202. https://doi.org/10.1006/jema.2001.0434

Giurco, D., Dominish, E., Florin, N., Watari, T., & McLellan, B. (2019). Requirements for Minerals and Metals for 100% Renewable Scenarios. In S. Teske (Ed.), *Achieving the Paris Climate Agreement Goals: Global and Regional 100% Renewable Energy Scenarios with Non-energy GHG Pathways for +1.5°C and +2°C* (pp. 437–457). Cham: Springer International Publishing. https://doi.org/10.1007/978-3-030-05843-2_11

Huertas, J. I., Camacho, D. A., & Huertas, M. E. (2012). Standardized emissions inventory methodology for open-pit mining areas. *Environmental Science and Pollution Research*, *19*(7), 2784–2794. https://doi.org/10.1007/s11356-012-0778-3

International Energy Agency. (n.d.). IEA, 2020. Retrieved September 3, 2021, from https://www.iea.org/reports/world-energy-outlook-2020

Jorquera, H., & Barraza, F. (2012). Source apportionment of ambient PM2.5 in Santiago, Chile: 1999 and 2004 results. *Science of The Total Environment*, *435–436*, 418–429. https://doi.org/10.1016/j.scitotenv.2012.07.049

Kaunda, R. B. (2020). Potential environmental impacts of lithium mining. *Journal of Energy & Natural Resources Law*, *38*(3), 237–244. https://doi.org/10.1080/02646811.2020.1754596

Kavouras, I. G., Koutrakis, P., Cereceda-Balic, F., & Oyola, P. (2001). Source Apportionment of PM10 and PM25 in Five Chilean Cities Using Factor Analysis. *Journal of the Air & Waste Management Association*, *51*(3), 451–464. https://doi.org/10.1080/10473289.2001.10464273

Klimont, Z., Cofala, J., Bertok, I., Amann, M., Heyes, C., & Gyarfas, F. (2002, December). Modeling Particulate Emissions in Europe. A Framework to Estimate Reduction Potential and Control Costs [Monograph]. Retrieved September 3, 2021, from http://pure.iiasa.ac.at/id/eprint/6712/

Klimont, Zbigniew, Kupiainen, K., Heyes, C., Purohit, P., Cofala, J., Rafaj, P., et al. (2017). Global anthropogenic emissions of particulate matter including black carbon. *Atmospheric Chemistry and Physics*, *17*(14), 8681–8723. https://doi.org/10.5194/acp-17-8681-2017

Lèbre, É., Stringer, M., Svobodova, K., Owen, J. R., Kemp, D., Côte, C., et al. (2020). The social and environmental complexities of extracting energy transition metals. *Nature Communications*, *11*(1), 4823. https://doi.org/10.1038/s41467-020-18661-9

Lorenz, M. O. (1905). Methods of Measuring the Concentration of Wealth. *Publications of the American Statistical Association*, *9*(70), 209–219. https://doi.org/10.2307/2276207

Masson-Delmotte, V., Zhai, P., Pirani, A., Connors, S. L., Péan, C., Berger, S., et al. (Eds.). (2021). Summary for policymakers. In *Climate Change 2021: The Physical Science Basis. Contribution of Working Group I to the Sixth Assessment Report of the Intergovernmental Panel on Climate Change*. Cambridge University Press.

Mohr, S., Giurco, D., Yellishetty, M., Ward, J., & Mudd, G. (2015). Projection of Iron Ore Production. *Natural Resources Research*, *24*(3), 317–327. https://doi.org/10.1007/s11053-014-9256-6

Mwaanga, P., Silondwa, M., Kasali, G., & Banda, P. M. (2019). Preliminary review of mine air pollution in Zambia. *Heliyon*, *5*(9), e02485. https://doi.org/10.1016/j.heliyon.2019.e02485

Pingitore, N. E., Jr. (2019). Unlocking a Strategic National Treasure: Multiple Critical and “Green” Minerals in Round Top Mt. Rhyolite, Far West Texas, U.S.A., *2019*, PA41C-1130.

Seefeldt, J. L. (2020). Lessons from the Lithium Triangle: Considering Policy Explanations for the Variation in Lithium Industry Development in the “Lithium Triangle” Countries of Chile, Argentina, and Bolivia. *Politics & Policy*, *48*(4), 727–765. https://doi.org/10.1111/polp.12365

Smith, S. J., van Aardenne, J., Klimont, Z., Andres, R. J., Volke, A., & Delgado Arias, S. (2011). Anthropogenic sulfur dioxide emissions: 1850–2005. *Atmospheric Chemistry and Physics*, *11*(3), 1101–1116. https://doi.org/10.5194/acp-11-1101-2011

The Paris Agreement | UNFCCC. (n.d.). Retrieved September 3, 2021, from https://unfccc.int/process-and-meetings/the-paris-agreement/the-paris-agreement

Tian, H. Z., Lu, L., Cheng, K., Hao, J. M., Zhao, D., Wang, Y., et al. (2012). Anthropogenic atmospheric nickel emissions and its distribution characteristics in China. *Science of The Total Environment*, *417–418*, 148–157. https://doi.org/10.1016/j.scitotenv.2011.11.069

US EPA, O. (2016, September 26). AP-42: Compilation of Air Emissions Factors [Other Policies and Guidance]. Retrieved September 3, 2021, from https://www.epa.gov/air-emissions-factors-and-quantification/ap-42-compilation-air-emissions-factors

Valero, A., Valero, A., Calvo, G., Ortego, A., Ascaso, S., & Palacios, J.-L. (2018). Global material requirements for the energy transition. An exergy flow analysis of decarbonisation pathways. *Energy*, *159*, 1175–1184. https://doi.org/10.1016/j.energy.2018.06.149

Watari, T., McLellan, B. C., Giurco, D., Dominish, E., Yamasue, E., & Nansai, K. (2019). Total material requirement for the global energy transition to 2050: A focus on transport and electricity. *Resources, Conservation and Recycling*, *148*, 91–103. https://doi.org/10.1016/j.resconrec.2019.05.015

Wu, Q. R., Wang, S. X., Zhang, L., Song, J. X., Yang, H., & Meng, Y. (2012). Update of mercury emissions from China’s primary zinc, lead and copper smelters, 2000–2010. *Atmospheric Chemistry and Physics*, *12*(22), 11153–11163. https://doi.org/10.5194/acp-12-11153-2012

Xue, Y., Wu, J., Feng, Y., Dai, L., Bi, X., Li, X., et al. (2010). Source Characterization and Apportionment of PM10 in Panzhihua, China. *Aerosol and Air Quality Research*, *10*(4), 367–377. https://doi.org/10.4209/aaqr.2010.01.0002

Supplementary Information

SI Text 1: Downscaling routine

This text describes the downscaling routine for IEA 26 regions to GAINS 180 regions for capacity addition data for solar PV and wind turbines.

GAINS has a downscaling routine to convert IEA energy generation by technology from its 26 regions to 180 GAINS regions (refs). However, capacity addition of solar PV and wind turbine is not represented using that routine. Here we estimate capacity addition (e.g. GW of Solar PV) from energy generation (e.g. kWh) from IEA 26 regions to GAINS 180 regions using equation S1.

$$\Delta CADD_{r,t} = \Delta CADD_{s,t} \frac{\Delta EADD_{r,t}}{\sum \Delta EADD_{r,t}} \quad \textbf{(S1)}$$

Where CADD is the estimated capacity addition in the GAINS region r in year t; EADD is the difference in energy generation between two time periods in GAINS region r in year t; and s is the IEA region the region GAINS region r belongs to.

For example, assume one IEA region, Asia, is made of two GAINS regions (India and China). Then, in a given year, the capacity addition of solar PV or wind turbine in India is assumed to be proportional to the fraction of Asia’s solar energy added in India.

Table S1: Metal intensities in solar, wind, and EVs, from Watari et al., 2019

Categories assumed in GAINS: **Red = Aluminum**, **Blue = Iron and steel**, and rest = NFME

Metal	Metal	Solar (ton / GW)	Wind (ton / GW)	EV (ton / unit)
Al	**Aluminum**	**33500**	**1372**	**0.127302**
Bo	Boron	0	1	0
Cd	Cadmium	0	0	0
Ce	Cerium	0	0	0
Cr	Chromium	1880	683	0.01185
Co	Cobalt	0	0	0.01346
Cu	Copper	3765	2497	0.0925
Dy	Dysprosium	0	16	0.000279
Er	Erbium	0	0	0
Gd	Gadolinium	0	0	0
Ga	Gallium	0	0	0
Ge	Germanium	0	0	0
In	Indium	0	0	0
Fe	**Iron (includes Steel)**	**1200000**	**119985**	**0.9095**
La	Lanthanum	0	0	0
Pb	Lead	39	0	0.00031
Li	Lithium	0	0	0.006768
Mg	Magnesium	0	0	0.0002
Mn	Manganese	0	57	0.03605
Mo	Molybdenum	200	335	0
Nd	Neodymium	0	148	0.000969
Ni	Nickel	1800	427	0.034589
Nb	Niobium	0	38	0
Pt	Platinum	0	0	0
Pr	Praseodymium	0	3	0.000001
Se	Selenium	0	0	0
Si	Silicon	6428	0	0
Ag	Silver	30	0	0
Te	Tellurium	0	0	0
Tb	Terbium	0	1	0
Sn	Tin	332	90	0
V	Vanadium	2	90	0
Zn	Zinc	1400	5450	0.0001

Table S2: Shows the absolute demand and as percent of IEA all-use for steel, aluminum, and non-ferrous non-aluminum for Business-As-Usual and Rapid Decarbonization pathways. All units in Million tons per year finished metal unless noted otherwise.

Steel

Business-As-Usual

	Metal demand (Million tons)			**Total**	**Total as percent of all-use production**
Year	**Solar**	**Wind**	**EV**		
2020	116.2	6.3	48.4	170.9	8.8
2025	146.5	7.1	25.2	178.8	8.3
2030	168.0	7.7	33.6	209.3	9.1
2035	186.8	8.0	41.4	236.3	9.7
2040	205.4	6.7	38.6	250.7	9.8
2045	209.5	7.0	34.6	251.2	9.4
2050	198.5	7.4	27.8	233.7	8.5

Rapid Decarbonization

	Metal demand (Million tons)			**Total**	**Total as percent of all-use production**
Year	**Solar**	**Wind**	**EV**		
2020	119.0	6.8	48.4	174.2	8.9
2025	255.4	12.3	29.5	297.2	13.2
2030	330.1	15.0	54.9	400.0	16.4
2035	342.2	15.2	78.7	436.0	17.3
2040	325.1	14.0	94.3	433.4	16.9
2045	273.1	12.4	85.8	371.3	14.6
2050	205.7	9.2	75.5	290.4	11.6

Aluminum

Business-As-Usual

	Metal demand (Million tons)			**Total**	**Total as percent of all-use production**
Year	**Solar**	**Wind**	**EV**		
2020	3.2	0.1	6.4	9.7	7.0
2025	4.1	0.1	3.3	7.5	4.9
2030	4.7	0.1	4.4	9.2	5.5
2035	5.2	0.1	5.5	10.8	5.8
2040	5.7	0.1	5.1	10.9	5.5
2045	5.8	0.1	4.6	10.5	5.0
2050	5.5	0.1	3.7	9.3	4.3

Rapid Decarbonization

	Metal demand (Million tons)			**Total**	**Total as percent of all-use production**
Year	**Solar**	**Wind**	**EV**		
2020	3.3	0.1	6.4	9.8	7.0
2025	7.1	0.1	3.9	11.2	7.4
2030	9.2	0.2	7.2	16.6	10.2
2035	9.6	0.2	10.4	20.1	11.6

2040	9.1	0.2	12.4	21.7	12.0
2045	7.6	0.1	11.3	19.1	10.4
2050	5.7	0.1	10.0	15.8	8.7

NFME

Business-As-Usual

	Metal demand (Million tons)			**Total**	**Total as percent of all-use production**
Year	**Solar**	**Wind**	**EV**		
2020	1.5	0.5	10.1	12.2	16.6
2025	1.9	0.6	5.3	7.8	10.7
2030	2.2	0.6	7.0	9.9	13.1
2035	2.5	0.7	8.7	11.8	15.2
2040	2.7	0.6	8.1	11.3	14.8
2045	2.8	0.6	7.2	10.6	12.9
2050	2.6	0.6	5.8	9.0	10.6

Rapid Decarbonization

	Metal demand (Million tons)			**Total**	**Total as percent of all-use production**
Year	**Solar**	**Wind**	**EV**		
2020	1.6	0.6	10.1	12.2	16.7
2025	3.4	1.0	6.2	10.6	13.9
2030	4.4	1.2	11.5	17.1	20.6
2035	4.5	1.2	16.4	22.2	25.4
2040	4.3	1.2	19.7	25.1	28.0
2045	3.6	1.0	17.9	22.6	24.0
2050	2.7	0.8	15.8	19.2	20.1

Table S3: Gini Index values for the sum of all metals across all technologies for the two decarbonization scenarios under two abatement pathways and two production regionalities.

	Actual Production Regionality			Self-Production Regionality	
	Projected Abatement			**Projected Abatement**	
	Decarbonization Pathway			**Decarbonization Pathway**	
	Business-As-Usual	**Rapid Decarbonization**		**Business-As-Usual**	**Rapid Decarbonization**
2025	0.59	0.56	**2025**	0.56	0.59
2030	0.54	0.57	**2030**	0.53	0.56
2035	0.50	0.57	**2035**	0.48	0.53
2040	0.46	0.55	**2040**	0.46	0.51
2045	0.47	0.53	**2045**	0.46	0.48
2050	0.54	0.54	**2050**	0.49	0.43
	Strictest Abatement			**Strictest Abatement**	
	Decarbonization Pathway			**Decarbonization Pathway**	
	Business-As-Usual	**Rapid Decarbonization**		**Business-As-Usual**	**Rapid Decarbonization**
2025	0.56	0.54	**2025**	0.56	0.59
2030	0.47	0.51	**2030**	0.55	0.58
2035	0.36	0.45	**2035**	0.54	0.58
2040	0.42	0.36	**2040**	0.64	0.68
2045	0.40	0.37	**2045**	0.66	0.68
2050	0.36	0.47	**2050**	0.70	0.67

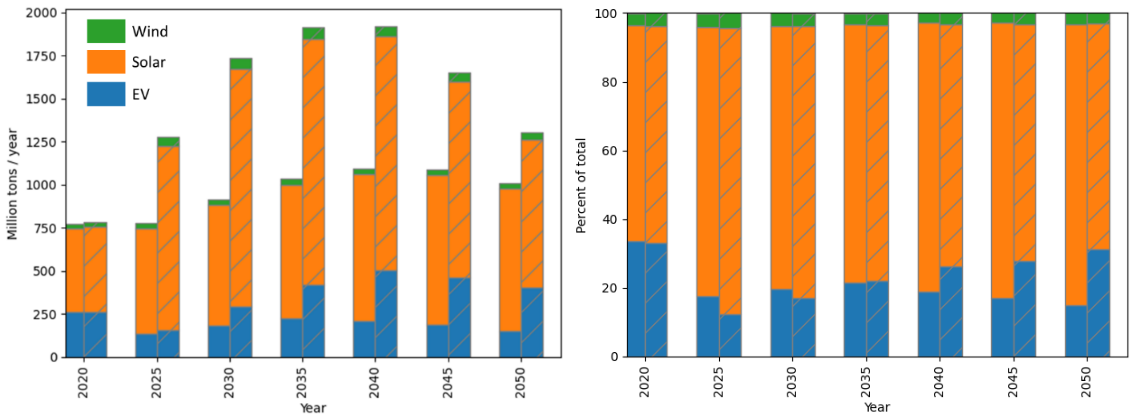

Figure S1: a) Metal demand, in million tons per year, by EVs, solar PVs, and Wind energy addition in Business-As-Usual (left sub-bars), and Rapid Decarbonization (right sub-bars, hatched); b) Same as (a) but percent of total.

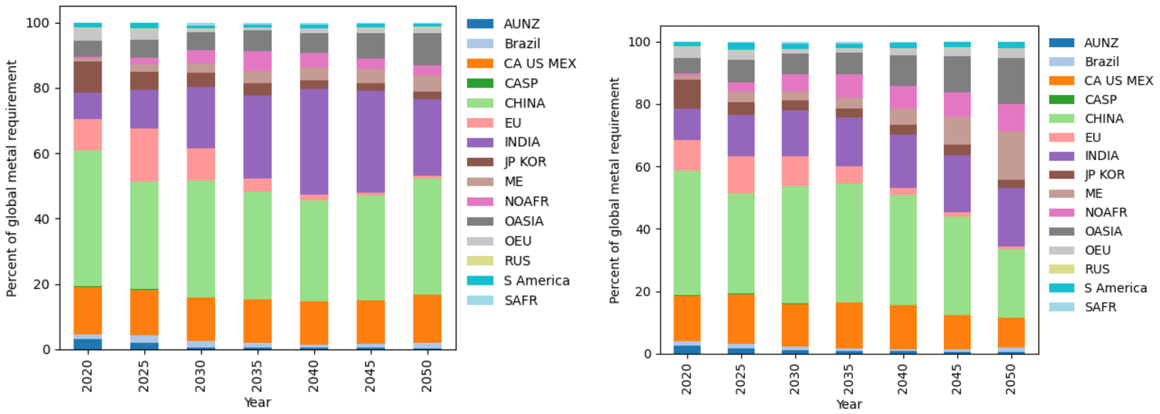

Figure S2: Relative metal demand by region for Business-As-Usual (left) and Rapid Decarbonization (right) for Solar PVs.

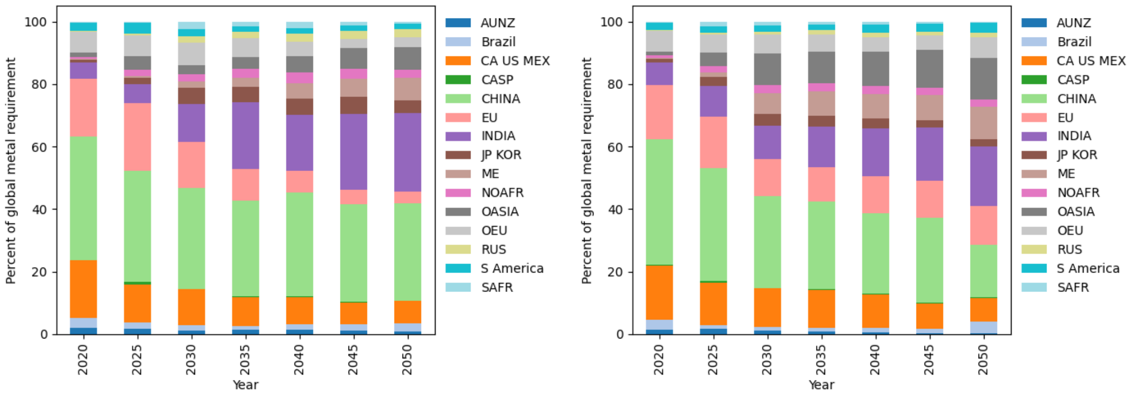

Figure S3: Relative metal demand by region for Business-As-Usual (left) and Rapid Decarbonization (right) for Wind turbines.

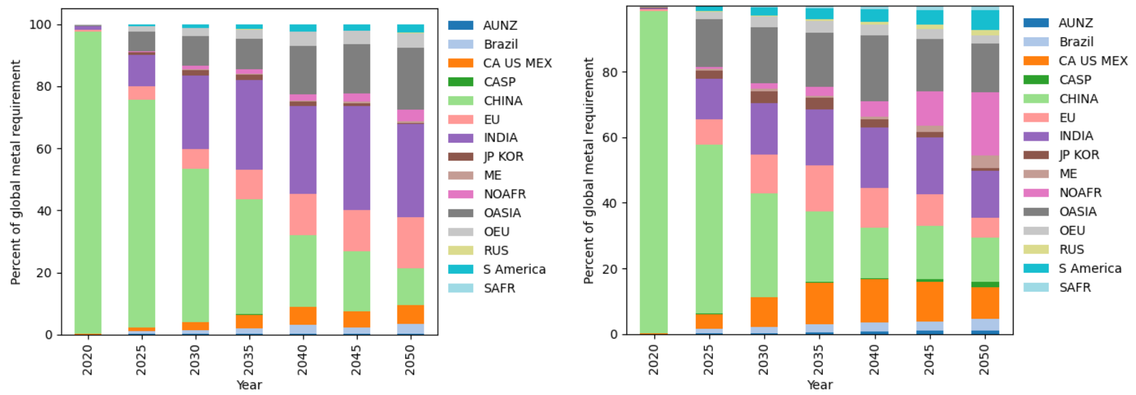

Figure S4: Relative metal demand by region for Business-As-Usual (left) and Rapid Decarbonization (right) for Electric vehicles.

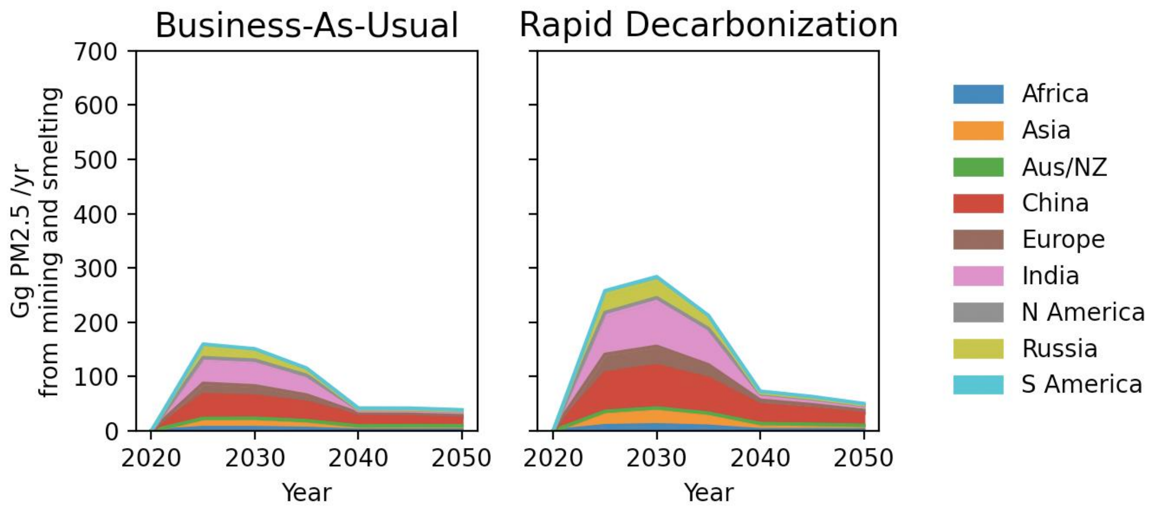

Figure S5: $PM_{2.5}$ emissions from metal mining and smelting toward making renewable energy devices in Business-As-Usual (a) and Rapid Decarbonization (b) scenarios by region with Strictest Abatement policies.

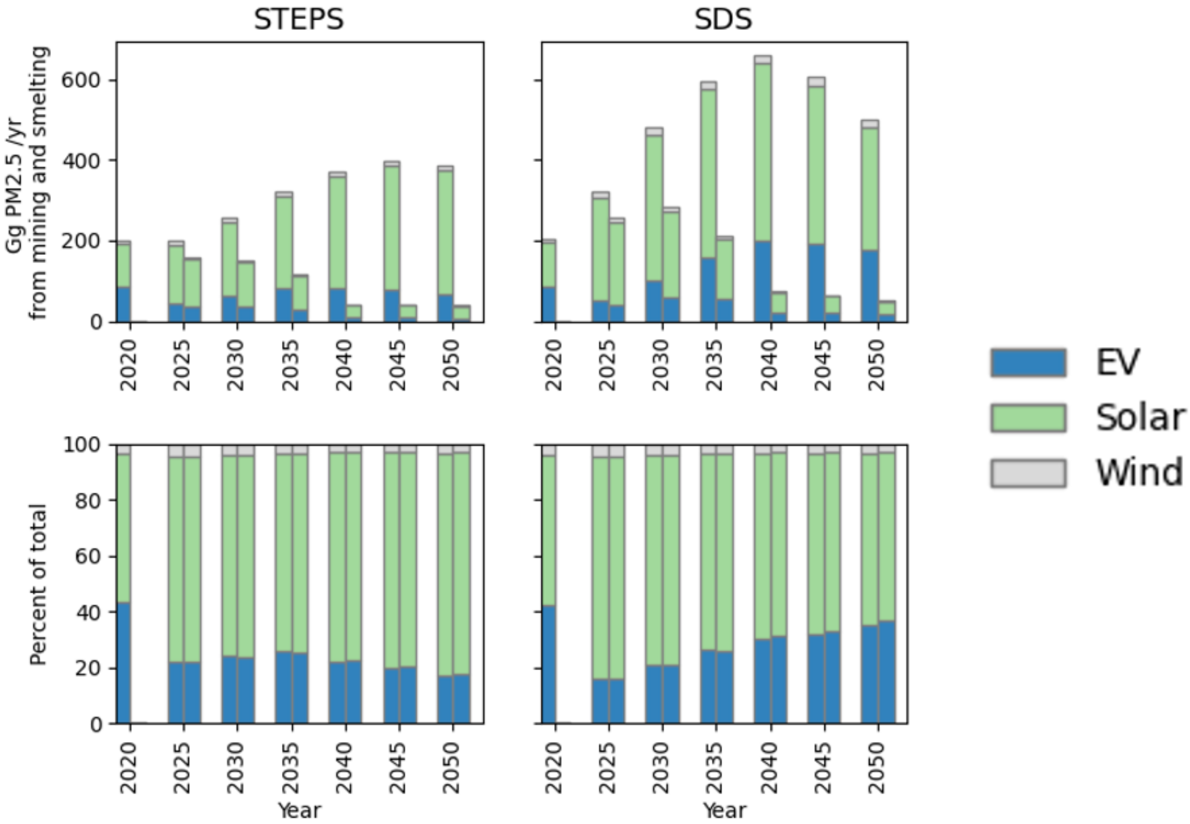

Figure S6: Absolute (top) and relative (bottom) $PM_{2.5}$ emissions from metal mining and smelting toward making renewable energy devices in Business-As-Usual (left) and Rapid Decarbonization (right) scenarios by technology. Left- and right sub-bars in each subplot show the Projected Abatement (current legislation, BAU abatement), and Strictest Abatement (stronger abatement) abatement policies, respectively. Strictest Abatement and Projected Abatement are same for 2020.

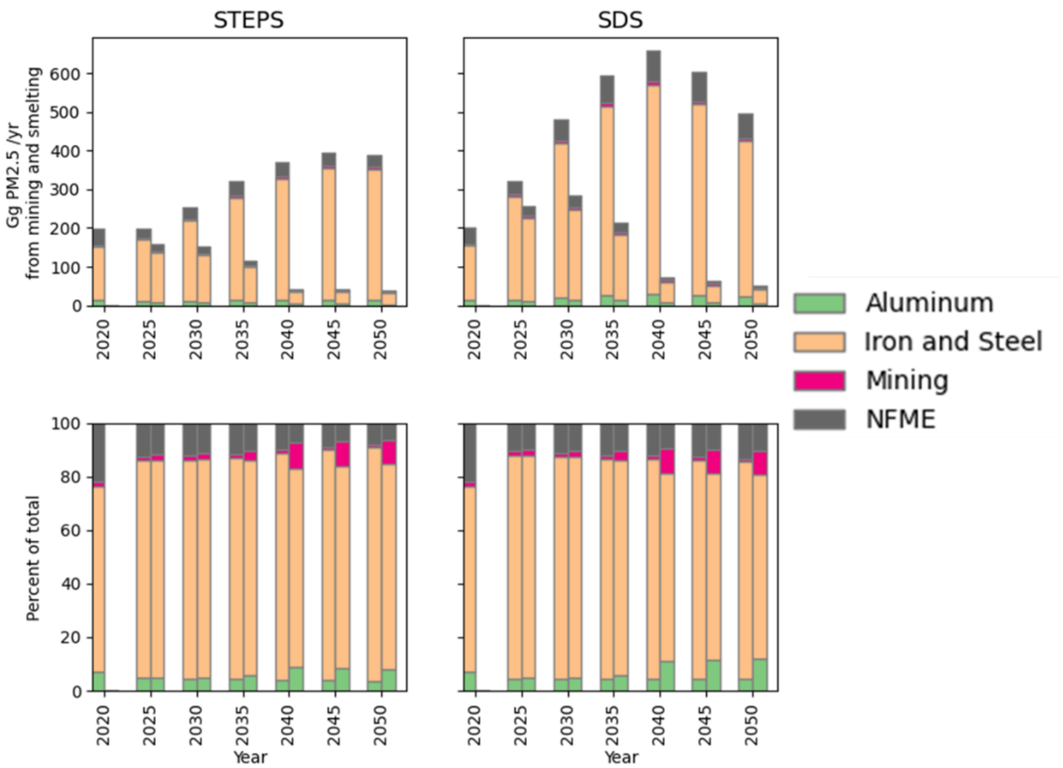

Figure S7: Absolute (top) and relative (bottom) $PM_{2.5}$ emissions from metal mining and smelting toward making renewable energy devices in Business-As-Usual (left) and Rapid Decarbonization (right) scenarios by metal and process. Left- and right sub-bars in each subplot show the Projected Abatement (current legislation, BAU abatement), and Strictest Abatement (stronger abatement) abatement policies, respectively. Strictest Abatement and Projected Abatement are same for 2020.

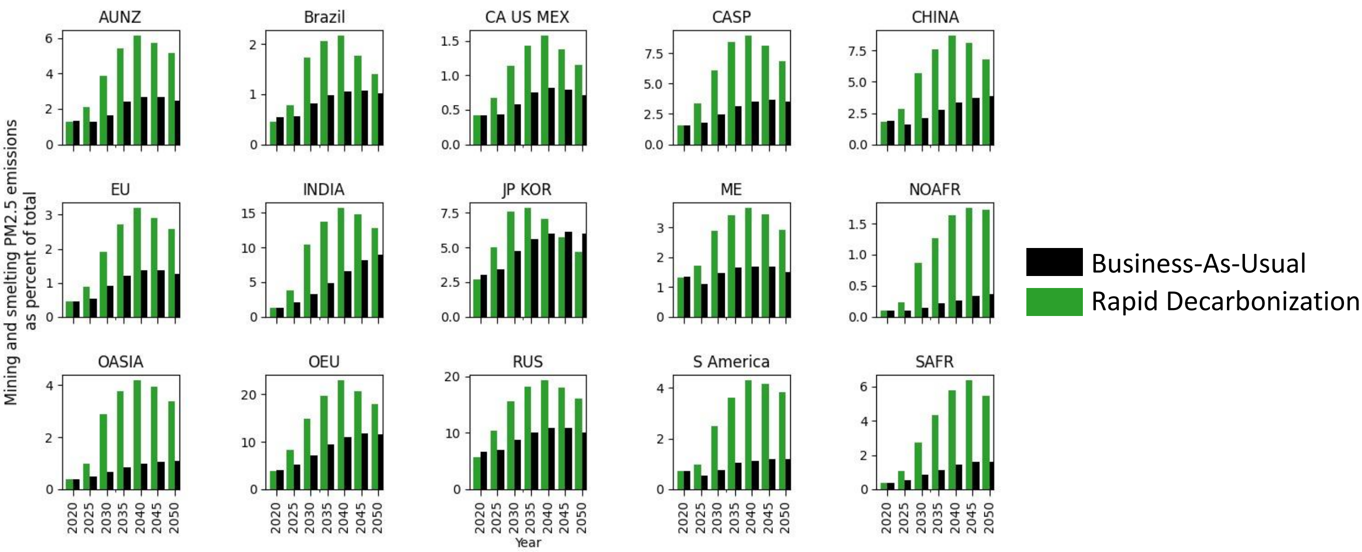

Figure S8: $PM_{2.5}$ emissions by mining and smelting to meet metal demand for renewables, shown as percent of total (mining and smelting and fossil fuel combustion) in the Business-As-Usual and Rapid Decarbonization scenarios for Projected Abatement.

Labels

1. AUNZ = Australia/New Zealand

2. CA US MEX = Canada, USA, Mexico

3. CASP = Central Asia

4. EU = European Union

5. JP KOR = Japan and Korea

6. ME = Middle East

7. NOAFR = North Africa

8. OASIA = Other Asia

9. OEU = Other Europe

10. RUS = Russia

11. S America = South America

12. SAFR = South Africa

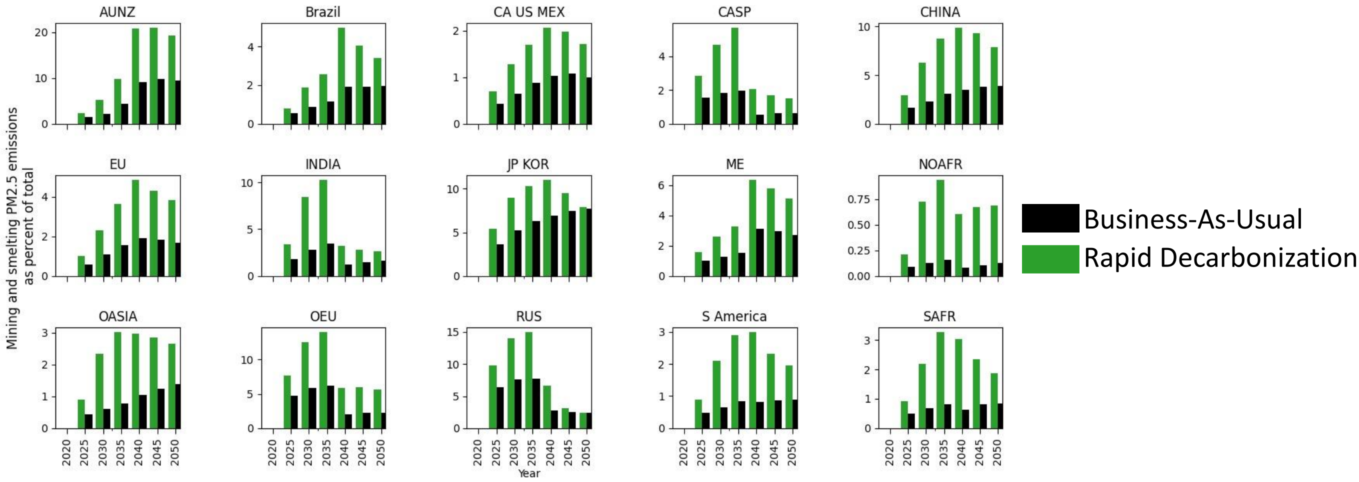

Figure S9: $PM_{2.5}$ emissions by mining and smelting to meet metal demand for renewables, shown as percent of total (mining and smelting and fossil fuel combustion) in the Business-As-Usual and Rapid Decarbonization scenarios for Strictest Abatement.

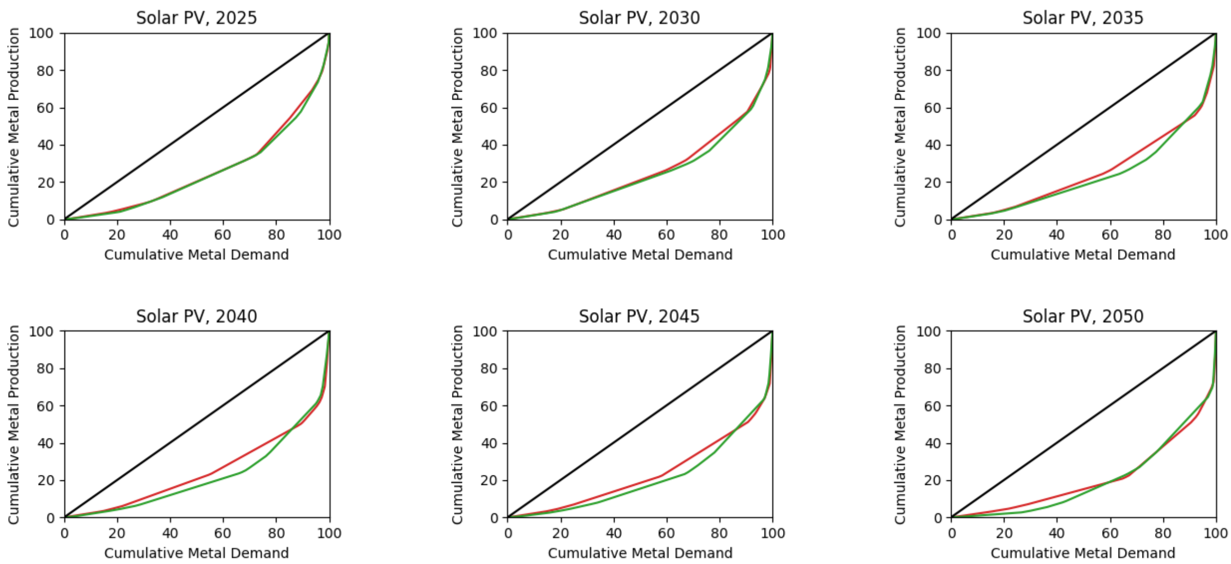

Figure S10: Global cumulative distribution of demand and supply of all metals in the Business-As-Usual (red) and Rapid Decarbonization (green) scenarios for the years 2025-2050 for Solar PV.

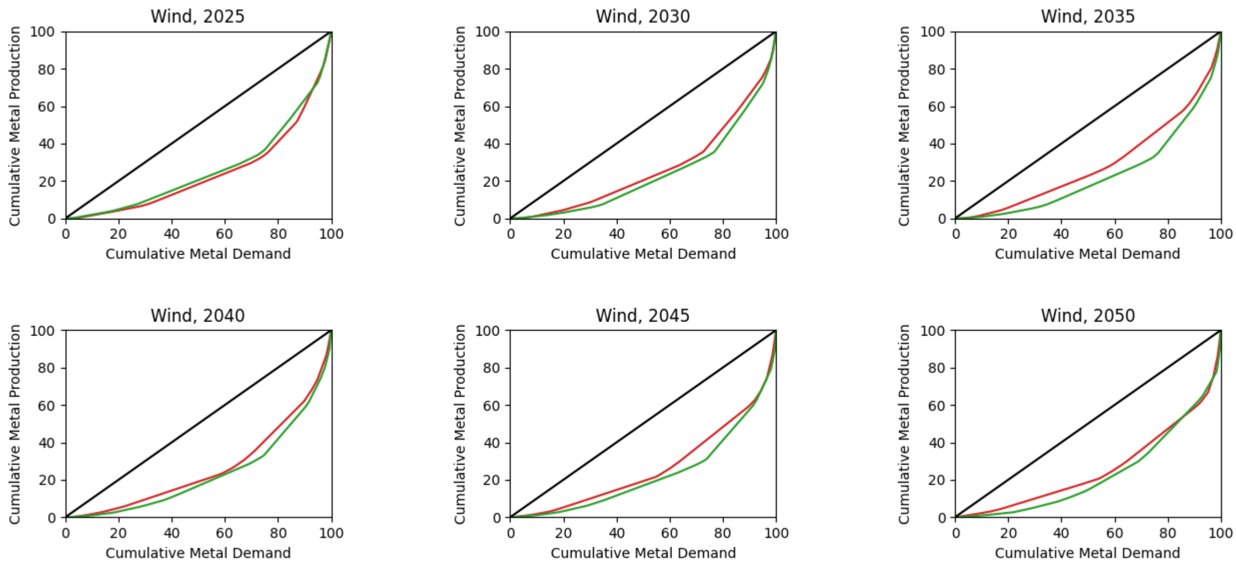

Figure S11: Global cumulative distribution of demand and supply of all metals in the Business-As-Usual (red) and Rapid Decarbonization (green) scenarios for the years 2025-2050 for Wind turbines.

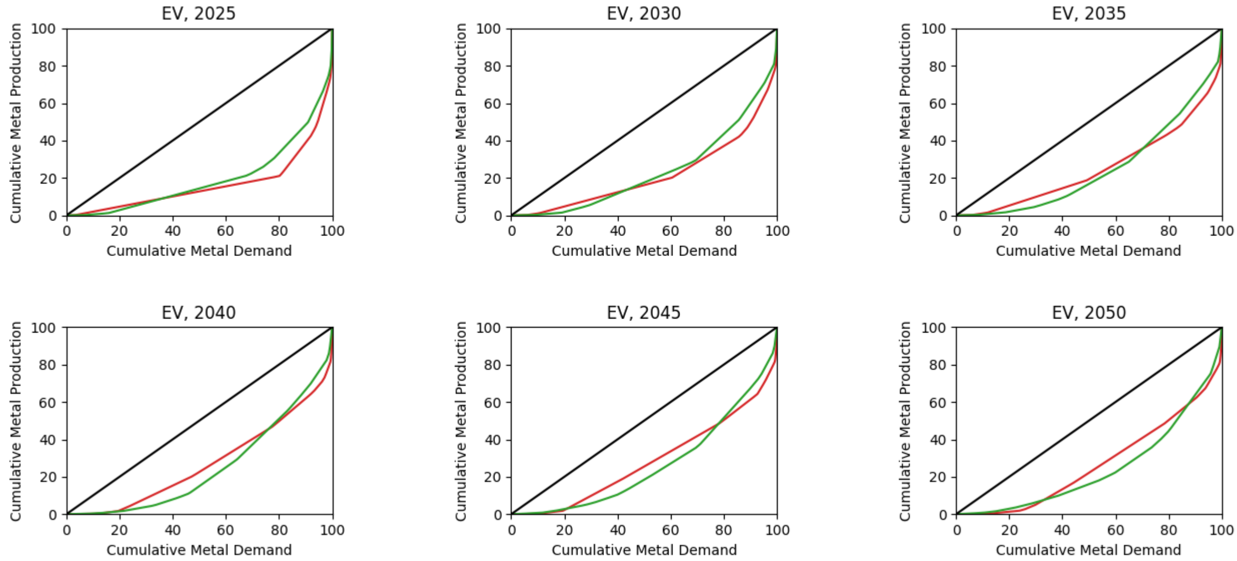

Figure S12: Global cumulative distribution of demand and supply of all metals in the Business-As-Usual (red) and Rapid Decarbonization (green) scenarios for the years 2025-2050 for Electric vehicles.

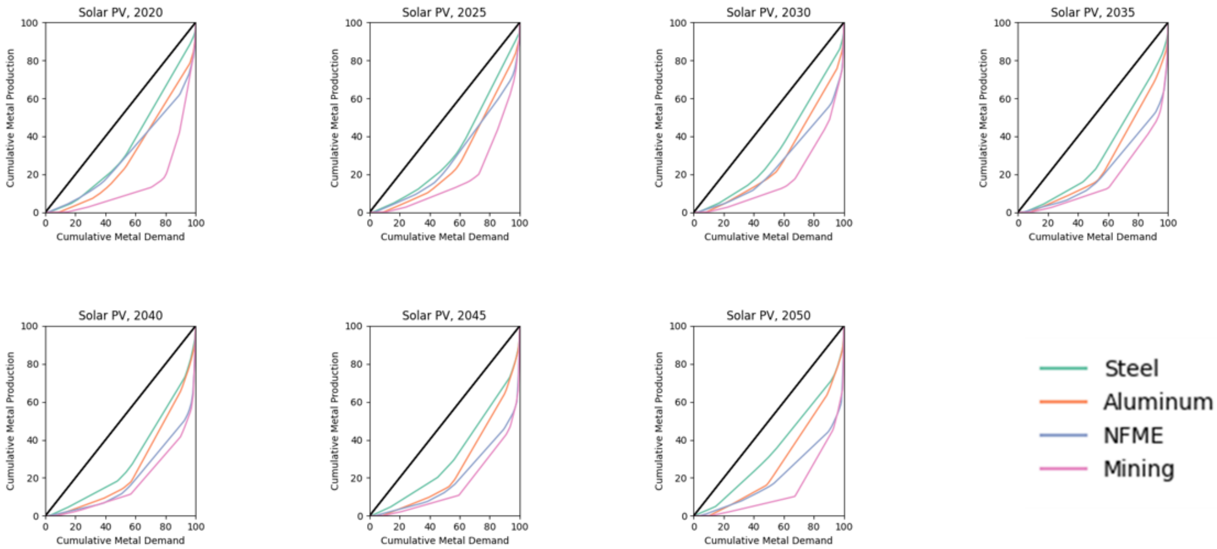

Figure S13: Global cumulative distribution of demand and supply of individual metals in the Business-As-Usual scenarios for the years 2020-2050 for Solar PV.

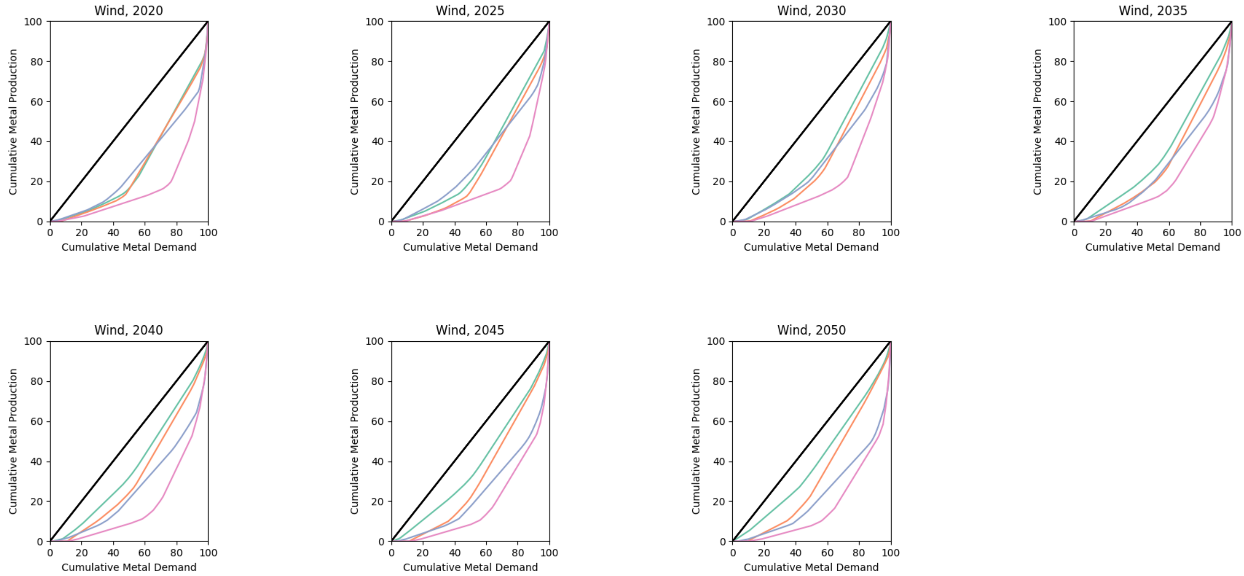

Figure S14: Global cumulative distribution of demand and supply of individual metals in the Business-As-Usual scenarios for the years 2020-2050 for Wind turbines. Labels same as Figure S13.

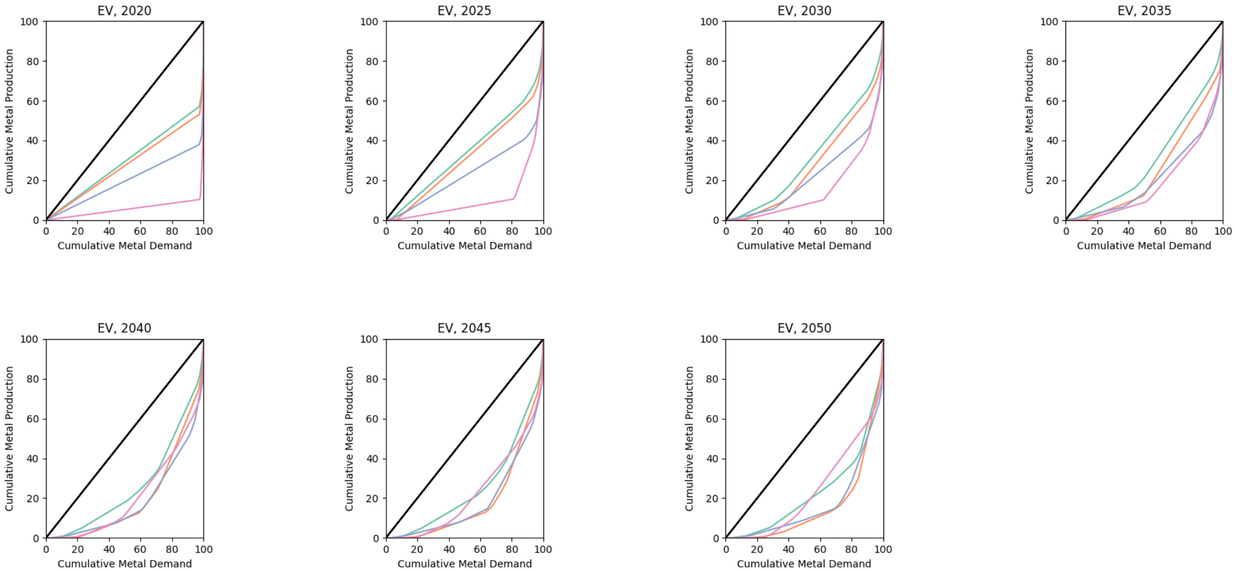

Figure S15: Global cumulative distribution of demand and supply of individual metals in the Business-As-Usual for the years 2020-2050 for Electric vehicles. Labels same as Figure S13.

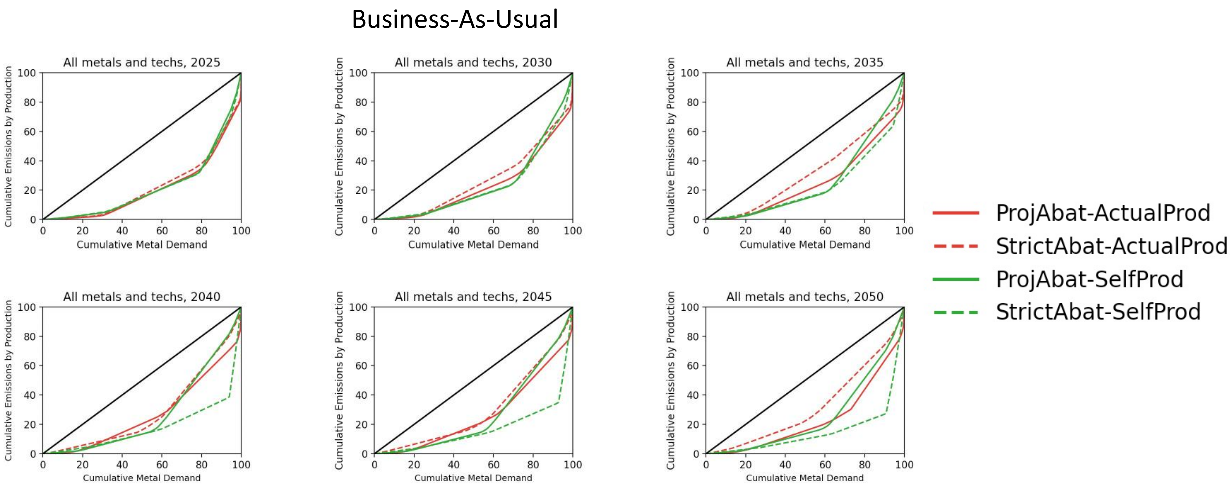

Figure S16: Global cumulative metal demand and emissions in the Business-As-Usual pathway, with Actual (red) and Self-Producing (green) scenarios in Projected Abatement (solid) and Strictest Abatement (green).

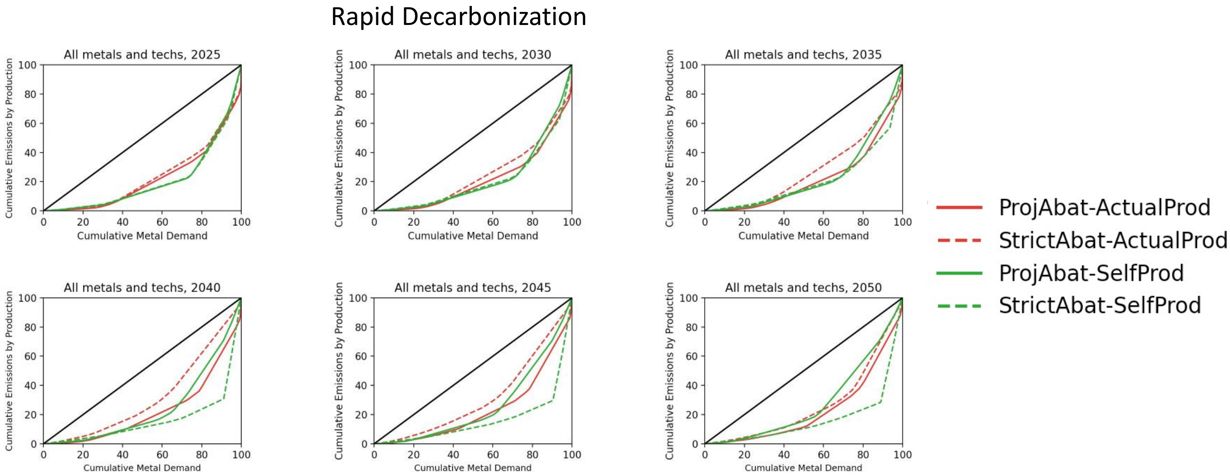

Figure S17: Global cumulative metal demand and emissions in the Rapid Decarbonization pathway, with Actual (red) and Self-Producing (green) scenarios in Projected Abatement (solid) and Strictest Abatement (dashed).